Journal of Materials Chemistry A

Accepted Manuscript

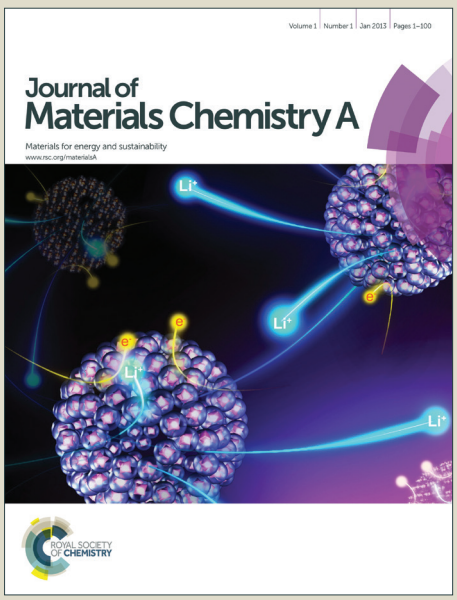

ROYAL SOCIETY OF CHEMISTRY

www.rsc.org/materialsA

Journal Name

RSCPublishing

ARTICLE

Relaxation is Key to Longer Life: Suppressed Degradation of P3HT Films on Conductive Substrates

Cite this: DOI: 10.1039/x0xx00000x

Yichen Zhao,[a] Abhilash Sugunan,*[a] Torsten Schmidt, Andrea Fornara,[b] Muhammet S. Toprak,[a] and Mamoun Muhammed[a]

Received 00th January 2012,
Accepted 00th January 2012

DOI: 10.1039/x0xx00000x

www.rsc.org/

ABSTRACT: Here we show a dependence of the degree of degradation of poly 3-hexylthiophene (P3HT) films on the conductivity of the supporting substrate. P3HT is widely used for organic solar cells and electronic devices because it allows simple, low cost fabrication and has potential for fabrication of flexible devices. However, P3HT is known to have a relatively low photo-stability and investigating the photo-degradation mechanism is an active research field. We find that P3HT films on conductive substrates show significantly retarded degradation and retain their chemical and morphological features when compared to similar films on glass substrates. This 'substrate effect' in retarding the degradation of P3HT films is evident even upon prolonged exposure to air for up to five months.

Introduction

Conjugated polymers have attracted a substantial interest in optoelectronic applications due to its semiconducting properties as well as simple and flexible processability.[1-4] Among the conjugated polymers, poly-(3-hexylthiophene); P3HT, is a very popular choice due to its high mobility of 0.1 $cm^2 V^{-1} s^{-1}$m.[5] As a p-type semiconductor polymer, P3HT is used as photo-active and/or hole transport layer in many optoelectronic devices, such as field effect transistors, light emitting diodes and solar cells.[6-14] In addition, by careful control of solvent evaporation, P3HT can be synthesised in the form of highly crystalline nanofibres, which have higher mobility than randomly organised films.[15]
However, like many other organic materials, P3HT degrades after a prolonged exposure to light and oxygen, resulting in the loss of interesting properties. Hence understanding the mechanisms of P3HT degradation and development of techniques to supress degradation is essential. Typically, degradation studies either involve spectroscopic investigation of P3HT films casted on glass substrates or completely assembled device performance is monitored over a period of time.[16,17] In the latter case, although practical information such as shelf life and active lifetime can be estimated, in-depth physical/chemical insight into the degradation mechanism is difficult. From the in-depth studies performed directly on P3HT films, it is known that under illumination, P3HT forms an excited state ($P3HT^*$), which subsequently forms a charge transfer complex (CTC) between $P3HT^*$ and oxygen. This CTC formation typically indicates the beginning of the degradation process.[18] Thus, it can be argued that when in contact with a conductive substrate, the P3HT* can be quenched, which in turn could slow down the degradation process.
Here, we show that degradation of P3HT was slower for films coated on conductive substrates compared to bare glass substrates, under various environments for over 5 months. An important implication of this 'substrate effect' is that optoelectronic devices using P3HT can be designed to have a longer lifetime with well-designed interfacial layers. It is noteworthy, that in most applications it is possible to place P3HT in intimate contact with a conductive substrate layer.

Experimental

Materials

Poly 3-hexylthiophene (P3HT) (regioregularity >95%) was purchased from Luminescence Technology Corp. (Taiwan, China). Anisole (anhydrous, 99.7%), normal glass slides and indium tin oxide (ITO) coated glass slides were purchased from Sigma Aldrich and used as received. Chloroform (99%) was purchased from VWR.

P3HT nanofibre synthesis

P3HT (12 mg) was added in anisole (6 mL) in a brown glass bottle and the solution was stirred for 10 minutes. Thereafter, chloroform (6 mL) was added to it and was placed in an ultrasonic bath until a clear solution was obtained. This solution was placed in a dark box with N_2 flow for 72 hours to obtain P3HT nanofibre solution.

P3HT film degradation experiment

A thick P3HT nanofibre film was prepared for the main degradation experiment. Two types of substrates; 1) normal glass; 2) indium tin oxide coated glass (ITO-glass) were used for the experiments. All the substrates, with similar surface area (ca. ~2.5 cm^2), were cleaned by ultrasonication in acetone for 10 minutes and dried in air. Thereafter, 100 µL of P3HT nanofibre solution was drop-casted and spread over each of the substrates. The casted solution was dried in a dark box under gentle N_2 flow, eventually forming a homogenous thick film of P3HT nanofibres over the substrates.
These samples were exposed to: 1) ambient light/air; 2) ambient light/N_2; 3) dark/air and 4) dark/N_2, as described in Table 1. The radiative flux of the ambient light was ~0.05 mW

cm^{-2}. The samples were analysed by UV-Vis spectroscopy at regular intervals for up to 5 months

Effect of different conductive substrates

To confirm that the 'substrate effect' was due to conductivity of substrates, a thin P3HT nanofibre film was prepared on three different types of substrate: 1) normal glass; 2) ITO-glass and 3) Au-glass (~30nm thin film of Au coated on glass substrates by evaporation). 100 µL of P3HT nanofibre solution was spin coated at 500 rpm for 10 s and then increasing to 3000 rpm for 120 s to form a uniform thin film. Afterwards the samples were exposed to a mercury lamp (~35 mW cm^{-2}) in air and optical spectra were measured every hour.

Characterisation

Transmission Electron Microscopy (TEM) imaging was done with a JEOL JEM-2100F operating at 200 kV. TEM samples were prepared by drop-casting a diluted P3HT fibre solution onto a carbon-coated copper grid.
Ultra violet-visible (UV-Vis) *absorption spectroscopy* was performed with a Perkin Elmer Lambda 750 spectrometer. *Fourier Transform Infrared* (FTIR) *spectroscopy* was performed with a Thermo Scientific Nicolet iS10 in attenuated total reflection (ATR) mode.
Atomic force microscopy (AFM) images were obtained using a JPK NanoWizard III AFM in tapping mode with a standard silicon tip (PPP-FMR, Nanosensors, drive frequency around 70 kHz, line scan rate 1 Hz).
X-ray diffractometry (XRD) was done with an Empyrean multipurpose high resolution X-ray diffractometer. Samples for XRD were prepared by drop-casting the P3HT fibre solution on glass substrates.
X-ray Photoelectron Spectroscopy (XPS) was performed using a Kratos AXIS Ultra^{DLD} X-ray photoelectron spectrometer. The samples were analysed using a monochromatic Al X-ray source and the analysed area was about 1 mm^2. The binding energy positions were calibrated by adjusting the C1-carbon peak to 285 eV. For high-resolution carbon spectra, the secondary carbon peaks were obtained by de-convolution of the shoulder in the C 1s spectra and the total amount of carbon is counted as 100% to quantify the relative percentage of un-oxidised carbon and oxidised carbon.
The radiative flux of light was measured by a broadband power/energy meter (Meller Griat 13PEM001).
Sheet resistivity of the substrates was measured by four-point probe station with Four Dimensions Inc, model 280. Single-site measurements were repeated at various positions on the substrates (error within 0.1%).

Results and discussion

We previously reported that P3HT can be slowly crystallised into free standing nanofibre structures by slow evaporation from a mixed solvent.[15] A representative TEM image of the P3HT nanofibres used in this experiment is shown in Figure 1a. The nanofibres are fairly uniform with average diameter of 17 nm. The fibre-like morphology is due to the crystal growth habit of P3HT during the slow crystallisation. The length of the fibres can be tuned with the total concentration of the mixed solution, while the fibre diameter is dependent on the ratio of the solvents in the mixed solvent system.[15]
High crystallinity of the P3HT nanofibres was confirmed with XRD by drop-casting P3HT nanofibres on a glass substrate (Figure 1b). A strong reflection is found at 2θ of 5.54°, which

Table 1. List of P3HT films on glass and ITO-glass substrate under different environments.

Substrate	Light, air	Light, N2	Dark, air	Dark, N2
Glass	P3HT-G1	P3HT-G2	P3HT-G3	P3HT-G4
ITO-glass	P3HT-I1	P3HT-I2	P3HT-I3	P3HT-I4

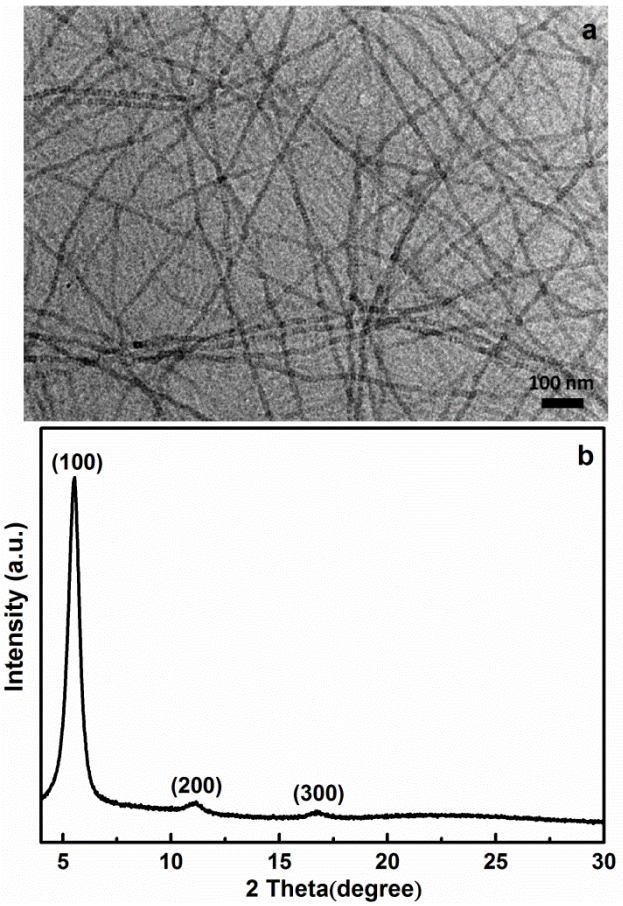

Figure 1. Fresh P3HT nanofibres characterised by TEM and XRD. a) Representative TEM image of a diluted P3HT nanofibre film on a carbon-coated copper grid, showing uniform diameter; b) X-ray diffraction of P3HT nanofibres on glass substrate, showing high crystallinity.

corresponds to the (100) plane with 15.9 Å interlayer spacing.[19]
P3HT nanofibres on glass substrate and ITO-glass substrate were obtained by drop casting and were subsequently exposed to different environments (Table 1). The optical absorption spectra of P3HT-G1 and P3HT-I1 were measured at regular intervals for up to 5 months (Figure 2). We observed that the intensity of the optical absorption peak at 520 nm decreased with time, indicating the degradation of P3HT. After 5 months, for P3HT-G1 the absorption intensity decreased by ca. 40% compared to its initial absorption intensity. In contrast, the degraded P3HT-I1 showed only 14% decrease compared to its initial absorption intensity. The absorption peak intensities at 520 nm were found to decrease linearly when plotted as function of time for all samples (Figure 3). The slope for P3HT-G1 is 0.004 per day, which is an order of magnitude higher than that of P3HT-I1 (0.0003 per day). Moreover, we found that samples on glass substrates consistently have a faster degradation than the samples on ITO-glass substrates in all the other environments. The major difference between glass substrate and ITO-glass substrate is its conductivity. We thus

conclude that the faster degradation is due to the lower conductivity of the glass substrate.

After the degradation experiment was completed, the two degraded P3HT-G1 and P3HT-I1 samples were compared by FTIR, shown in Figure 4. A fresh P3HT film (fresh-sample) was also prepared and measured as a reference. The relevant peaks and their assignments are listed in Table 2. We found that in both cases peaks 1–4, representing C=C stretching in thiophene rings, disappeared.[20,21] The peaks attributed to symmetric C=C ring stretching (peak 5), asymmetric C=C ring stretching (peak 6), and C-H stretching in the thiophene ring (peak 7, 8) dramatically decreased in both cases.[22] However, we found that peak 11 at 722 cm^{-1}, corresponding to vibrations of S atoms in the thiophene rings, was still present in both cases.[23] Therefore, we conclude that thiophene rings have been affected but the ring structure still exists when the degradation experiment was finished for both the cases.

Peak 9 in the fresh-sample, assigned to aromatic C-H out of plane vibrations in the thiophene ring, is sharp and narrow.[24] Interestingly, we observe a new peak (peak 10) in sample P3HT-G1 at 840 cm^{-1}, resulting in a broad peak between 800 – 850 cm^{-1} (Figure 4f). Peak 10 is assigned to C-H out of plane vibrations in an aliphatic alkene.[21] It is notable that there is no aliphatic alkene in the original P3HT monomer. According to Abdou's theory, the formation of CTC from excited P3HT ($P3HT^*$) is the beginning of the degradation.[18] The CTC is formed by reaction with oxygen, which causes one of the double bond from the thiophene ring to shift to the side chain. This can explain the appearance of peak 10 in the case of P3HT-G1.[25] On the other hand, in sample P3HT-I1 the excited P3HT is quickly quenched by the ITO layer back to the ground state, making it more resistant to oxygen. Therefore, peak 10 only appears as a weak shoulder in P3HT-I1. Thus, we conclude that peak 10 is a characteristic peak indicating the onset of degradation of P3HT.

The characteristic peak 10 is compared for all glass substrates

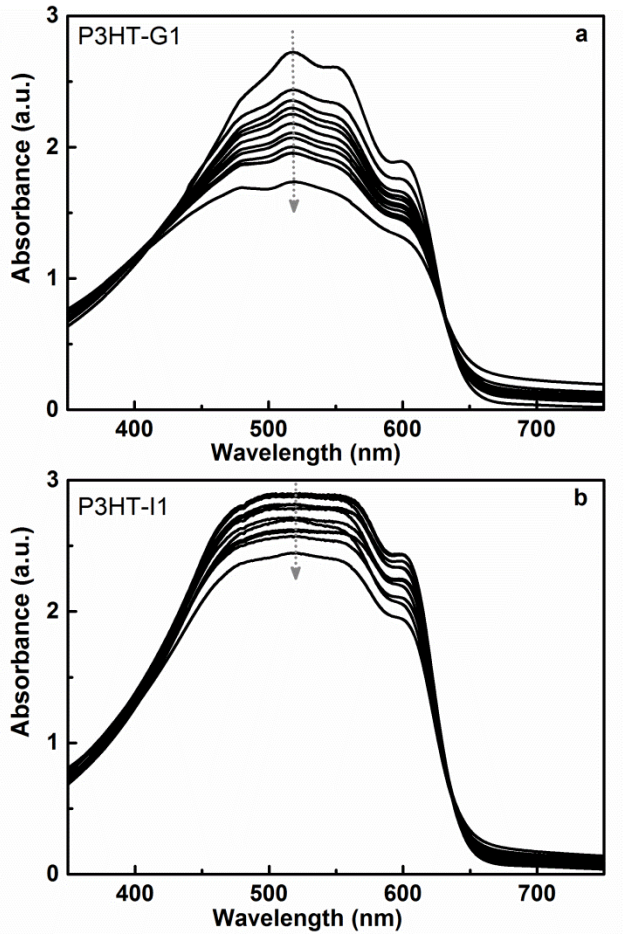

Figure 2. Evolution of absorption spectra of P3HT film on a) glass substrate and b) ITO-glass substrate measured for 5 months.

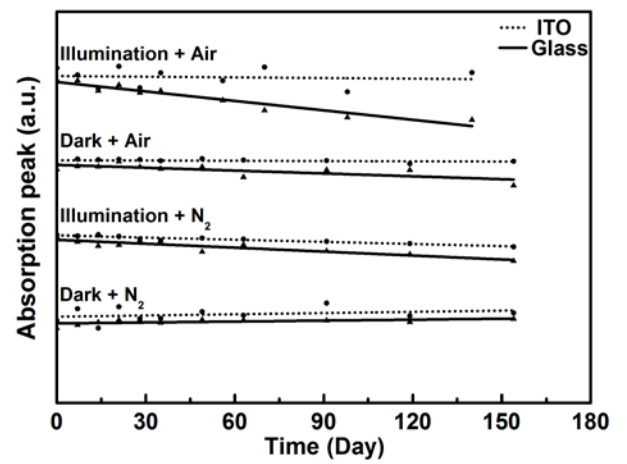

Figure 3. Trace of absorption peak intensity (λ = 520 nm) of P3HT films over time on glass and ITO-glass substrates under different environments.

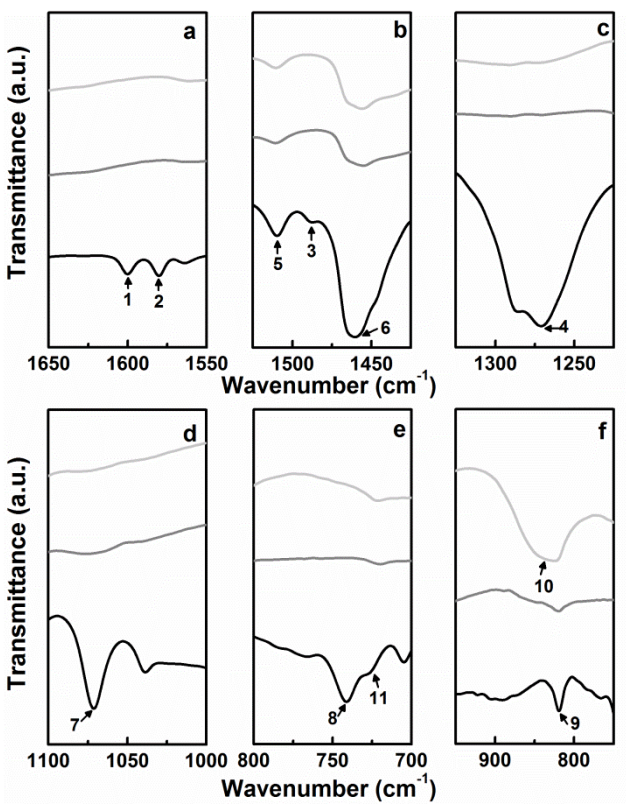

Figure 4. Relevant peaks in the FTIR spectra of P3HT films after 5 months of exposure to light and air. The appearance of peak 10 is indicative of onset of degradation. Light grey line: P3HT-G1, grey line: P3HT-I1 and black line: fresh-sample. The functional groups assigned for each of these peaks are listed in Table 2.

Table 2. Relevant FTIR peaks in Figure 4 and their assignments.

Peak No.	Wavenumber (cm-1)	Assignments	Note
1, 2, 3, 4	1597, 1579, 1458, 1260	C=C stretching in thiophene ring	Disappeared
5	1507	Symmetric C=C ring stretching	Decreased
6	1458	Asymmetric C=C ring stretching	Decreased
7,8	1069, 740	C-H stretching in thiophene ring	Decreased
9	817	Aromatic C-H out of plane vibration in thiophene ring	Unaffected
10	840	Aliphatic C-H out of plane vibration in alkene	Appeared only in P3HT-G1
11	722	Vibration of S	Unaffected

and ITO-glass substrates (Figure 5). We notice the appearance of the peak in all samples with glass as substrate (Figure 5a), indicating degradation. On the other hand, the characteristic peak appears only as a weak shoulder in all samples with ITO-glass as substrate (Figure 5b). Interestingly, the P3HT films on ITO-glass substrate that was exposed to air and illumination (P3HT I1) also showed very less degradation, suggesting that the 'substrate effect' in retarding the degradation is valid even upon prolonged exposure to air and illumination. The observations from Figure 4 and Figure 5 are consistent with the conclusions from Figure 2 and Figure 3, confirming that the samples on ITO-glass show significantly less degradation compared to the samples on glass.

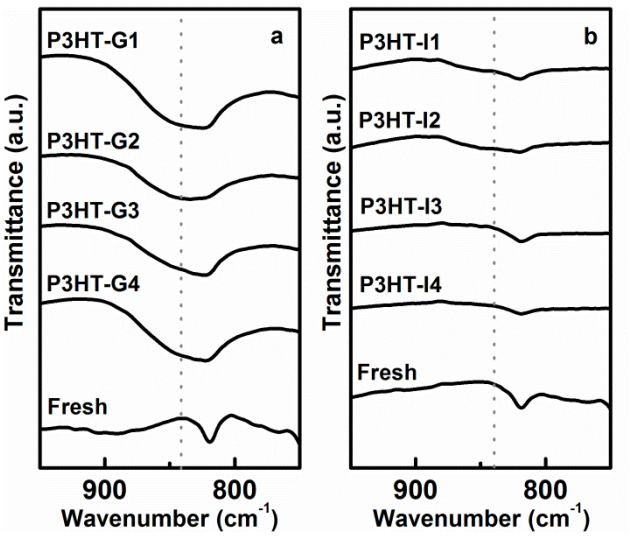

Figure 5. Comparison of the characteristic peak in the FTIR spectra of P3HT films on a) glass substrate and b) ITO-glass substrate. The characteristic peak is strong in all the glass samples, while it appears as a weak shoulder in the samples on ITO-glass. The dotted line is a guide to the eye marking the position of the characteristic peak at wavenumber 840 cm^{-1}.

We then studied the morphological and chemical effects of the degradation process by AFM and XPS, respectively. We selected P3HT-G1 (the 'most degraded' sample) and P3HT-I4 (the 'least degraded' sample) for this study. These samples were compared with the 'fresh-sample'.

AFM height images of the three samples, taken in tapping mode, are shown in Figure 6. As expected from previous analyses, P3HT-G1 (Figure 6a) appeared dramatically different from both P3HT-I4 and the fresh-sample (Figure 6b & c). While the fresh-sample and P3HT-I4 retained their nanofibrous network structure and showed a contiguous film-like appearance, P3HT-G1 showed a bumpy, island-like structure. This discontinuous structure of P3HT-G1 might lead to poor conductivity of the film due to absence of a percolation pathway for the charge carriers. On the other hand, P3HT-I4 and the fresh-sample are similar in surface morphology which suggests that P3HT-I4 may retain its original conductivity after a long period of time.

For a detailed chemical analysis, P3HT-G1, P3HT-I4 and the fresh-sample were analysed by XPS. The obtained relative surface atomic compositions are listed in Table 3. We found that P3HT-I4 and the fresh-sample have a similar surface atomic composition of carbon and oxygen; whereas there is 30% reduction in carbon and 75% increase in oxygen on the surface of P3HT-G1. The core level carbon and oxygen spectra for these three samples are shown in Figure 7 and the details are

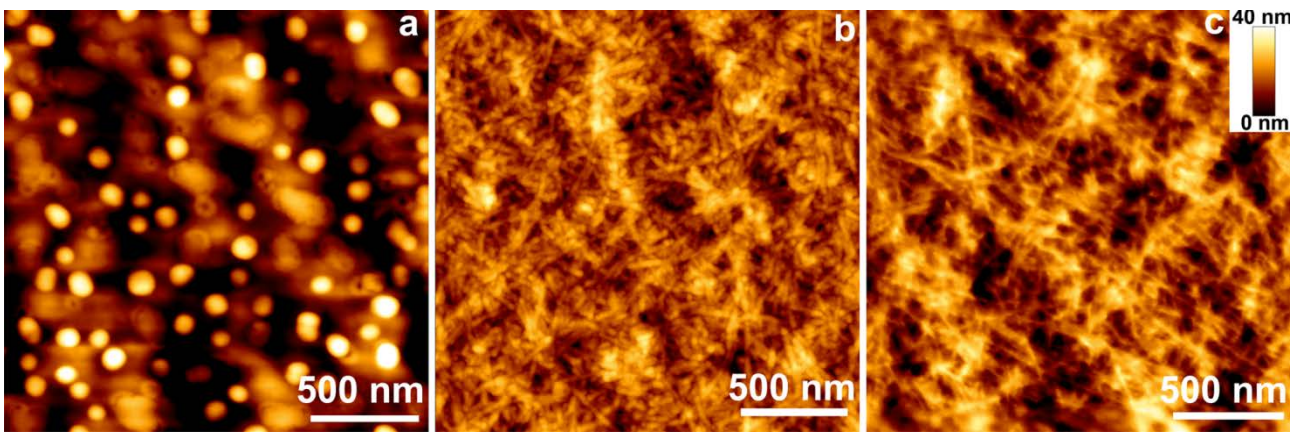

Figure 6. AFM height images of P3HT nanofibres deposited on different substrates. a) P3HT-G1; b) P3HT-I4; and c) fresh-sample. P3HT-G1 shows an island-like surface morphology, whereas P3HT-I4 and the fresh-sample show a contiguous nanofibrous network structure.

Table 3: Relative surface composition in atomic % from XPS spectra of P3HT films.

Sample	Atomic %		
	C	O	S
P3HT – G1	57.5	31.4	5.0
P3HT – I4	84.4	7.7	5.6
Fresh sample	84.7	8.4	4.6

Table 4: Chemical shifts in the high-resolution carbon XPS spectra of P3HT films.

Sample	C tot= 100%			
	C1a)	C2b)	C3d)	C4d)
P3HT – G1	65.1	12.8	8.3	13.8
P3HT – I4	91.3	3.0	3.6	2.1
Fresh sample	90.6	4.0	3.4	2.0

a) C1: C-C, C=C, C-H;

b) C2: C-O, C-O-C;

c) C3: O-C-O, C=O, N-C-O, N-C=O;

d) C4: C(=O)OH, O-C=O, N-C(=O)-N

listed in Table 4. Both P3HT-I4 and the fresh-sample have ~ 90% of total as C1- carbon which indicates un-oxidised organic carbon bonds (Figure 7b & c), whereas there is only 65% of C1-carbon in the P3HT-G1 sample.[26] Correspondingly, a higher percentage of C2-, C3- and C4- carbon, which indicates oxidised organic carbon bonds, is detected in the P3HT-G1 sample (Figure 7a). The secondary carbon peaks were obtained by de-convolution of the shoulder in the C 1s spectra. This is consistent with our FTIR results, showing that P3HT-G1 was more vulnerable to reaction with oxygen, leading to a more serious degradation. As a further confirmation, we also found that the intensity of core level spectra of O1s (Figure 7d) in P3HT-G1 is 3 times more than that of P3HT-I4 and the fresh-sample.

It is known from the literature that performance decay of polymer solar cells concomitantly shows a physical morphology change in the active layer.[27] We can now link this morphology change to a chemical degradation of the P3HT molecule. It is evident that by suppressing the chemical degradation, we can avoid this change in morphology. To avoid the chemical degradation, maintaining an intimate contact of the P3HT layer with a conductive layer is required, and is probably more important than sealing the device to exclude oxygen.

To confirm whether the 'substrate effect' is due to some ITO specific interactions or the conductivity of the substrate, an additional experiment was done. A thin film of P3HT nanofibres was spin-coated on glass substrate and two types of conductive substrates: ITO-glass and Au-glass. The samples were then exposed to a bright light source in air. The optical absorption maxima were plotted with respect to time (Figure 8). We found that P3HT film on the Au-glass substrate showed a much slower degradation rate compared to the film on the glass substrate (slope: 0.007 per hour and 0.015 per hour, respectively). Interestingly, the degradation rate of P3HT film on the Au-glass substrate was even slower than the degradation rate of film on the ITO-glass (slope: 0.01 per hour). This was expected since the sheet resistivity of ITO-glass (~80 Ω sq^{-1}) is higher than that of Au-glass (~2 Ω sq^{-1}). The time-scale for the degradation was much shorter in this experiment mainly due to

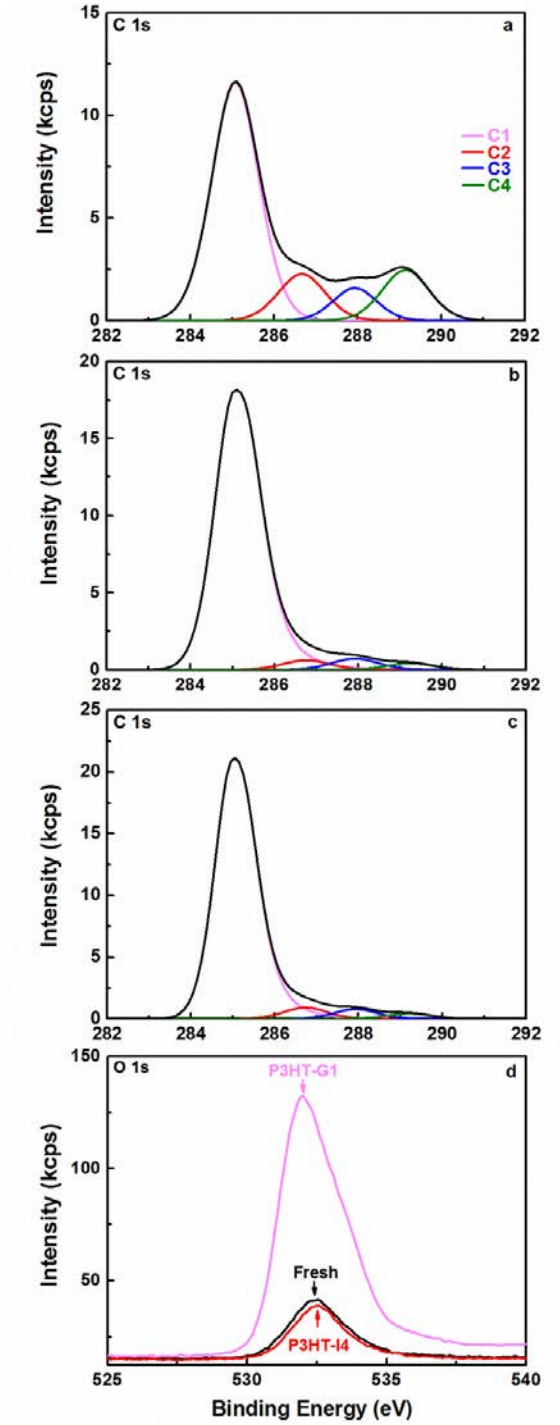

Figure 7. XPS spectra of P3HT samples showing core level C 1s of a) P3HT-G1, b) P3HT-I4 and c) fresh-sample. d) Oxygen 1 s spectra for the three samples.

exposure to much higher radiative flux (~700 times) and thinner layer of P3HT. This confirms that the 'substrate effect' is not specific to ITO-glass and is valid for other conductive substrates as well.

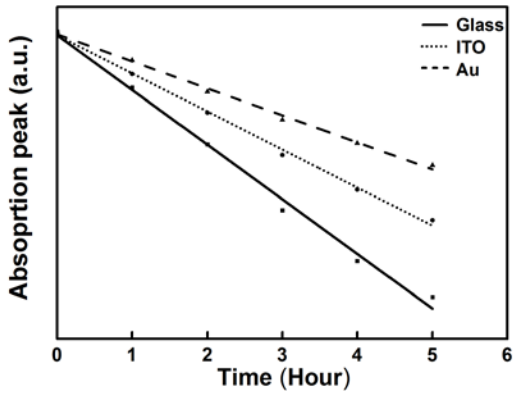

Figure 8. Effect of different conductive substrates: the trace of absorption peak intensity of P3HT thin layer on glass, ITO-glass and Au-glass, under a bright light source in air. All lines were shifted to the same starting point for comparison.

It is noteworthy that here the metal deposition was done directly on the glass substrate. It is difficult to speculate if the 'substrate effect' would still be observed if any interfacial doping layer is formed during metal deposition over polymers. [28,29] This would be an interesting future experiment.
In this work, high work function materials (Au, ITO) were studied. Another future experiment would be to investigate this 'substrate effect' of P3HT when placed in contact with low work function metals.

Conclusions

In summary, we report for the first time that the degradation of P3HT is significantly affected by the conductivity of the substrate on which it is deposited. Spectroscopic comparison shows a greatly suppressed degradation for P3HT deposited on conductive substrates (ITO-glass and Au-glass) compared to bare glass substrate. We attribute this substrate effect to the quenching of excited-state P3HT by the conductive layer preventing further reaction by oxygen. We identified a characteristic peak of the degradation process at wavenumber 840 cm^{-1} in the FTIR spectrum. This was confirmed by XPS, which showed a higher percentage of oxidised carbon and higher intensity of oxygen peaks in the case of P3HT films on glass substrates. In addition, the degradation process changes the morphology from a contiguous fibrous network to discontinuous islands in the case of the P3HT films on glass substrate, while on the ITO-glass substrates the film morphology was largely unchanged. We can thus conclude that the well-known chemical and physical degradation of P3HT films can be retarded significantly when the P3HT film is in contact with a conductive layer.

Acknowledgements

Authors acknowledge Xi Chen and Min Yan from Optics and Photonics Division in KTH for valuable discussion, supplying the Au-glass substrate and help with substrate conductivity measurements. Authors also acknowledge the valuable suggestions from anonymous reviewers. Authors acknowledge the financial support from Swedish Foundation for Strategic Research (SSF, Grant no EM11-0002).

Notes and references

[a] Department of Materials and Nano Physics, School of Information and Communication Technology, KTH Royal Institute of Technology, Isafjordsgatan 22, Kista, SE-164 40, Sweden.
*corresponding author: abhilash@kth.se
[b] Chemistry, Materials and Surfaces Unit, SP Technical Research Institute of Sweden, Stockholm, Box 5607, SE-114 86, Sweden.

1. J. L. Brusso, M. R. Lilliedal, and S. Holdcroft, *Polym. Chem.*, 2011, **2**, 175–180.
2. J.-T. Chen and C.-S. Hsu, *Polym. Chem.*, 2011, **2**, 2707–2722.
3. A. J. Moulé and K. Meerholz, *Adv. Mater.*, 2008, **20**, 240–245.
4. F. Boon, N. Hergué, G. Deshayes, D. Moerman, S. Desbief, J. De Winter, P. Gerbaux, Y. H. Geerts, R. Lazzaroni, and P. Dubois, *Polym. Chem.*, 2013, **4**, 4303–4307.
5. W. U. Huynh, J. J. Dittmer, and A. P. Alivisatos, *Science*, 2002, **295**, 2425–2427.
6. H. Zhou, L. Yang, and W. You, *Macromolecules*, 2012, **45**, 607–632.
7. K. Schmoltner, F. Schlütter, M. Kivala, M. Baumgarten, S. Winkler, R. Trattnig, N. Koch, A. Klug, E. J. W. List, and K. Müllen, *Polym. Chem.*, 2013, **4**, 5337–5344.
8. Q. Pei, Y. Yang, G. Yu, C. Zhang, and A. J. Heeger, *J. Am. Chem. Soc.*, 1996, **118**, 3922–3929.
9. D. Chen, A. Nakahara, D. Wei, D. Nordlund, and T. P. Russell, *Nano Lett.*, 2011, **11**, 561–567.
10. M. D. Heinemann, K. von Maydell, F. Zutz, J. Kolny-Olesiak, H. Borchert, I. Riedel, and J. Parisi, *Adv. Funct. Mater.*, 2009, **19**, 3788–3795.
11. C. P. Liu, H. E. Wang, T. W. Ng, Z. H. Chen, W. F. Zhang, C. Yan, Y. B. Tang, I. Bello, L. Martinu, W. J. Zhang, and S. K. Jha, *Phys. Status Solidi*, 2012, **249**, 627–633.
12. M. A. Niedermeier, M. Rawolle, P. Lellig, V. Kçrstgens, E. M. Herzig, A. Buffet, S. V. Roth, J. S. Gutmann, T. Frçschl, , N. H sing, and P. Müller-Buschbaum, *ChemPhysChem*, 2013, **14**, 597 – 602.
13. G. Kaune, E. Metwalli, R. Meier, V. Körstgens, K. Schlage, S. Couet, R. Röhlsberger, S. V. Roth, and P. Müller-Buschbaum, *ACS Appl. Mater. Interfaces*, 2011, **3**, 1055–1062.
14. M. A. Ruderer, C. Wang, E. Schaible, A. Hexemer, T. Xu, and P. Müller-Buschbaum, *Macromolecules*, 2013, **46**, 4419–4501.
15. Y. Zhao, A. Sugunan, D. B. Rihtnesberg, Q. Wang, M. S. Toprak, and M. Muhammed, *Phys. Status Solidi*, 2012, **9**, 1546–1550.
16. B. Conings, S. Bertho, K. Vandewal, A. Senes, J. D'Haen, J. Manca, and R. A. J. Janssen, *Appl. Phys. Lett.*, 2010, **96**, 163301–3.
17. E. T. Hoke, I. T. Sachs-Quintana, M. T. Lloyd, I. Kauvar, W. R. Mateker, A. M. Nardes, C. H. Peters, N. Kopidakis, and M. D. McGehee, *Adv. Energy Mater.*, 2012, **2**, 1351–1357.
18. M. S. A. Abdou, F. P. Orfino, Z. W. Xie, M. J. Deen, and S. Holdcroft, *Adv. Mater.*, 1994, **6**, 838–841.
19. L. Li, G. Lu, and X. Yang, J. Mater. Chem., 2008, 18, 1984–1990.
20. R. M. Silverstein and F. X. Webster, *Spectrometric Identification of Organic Compounds*, Wiley, New York, 6th edn., 1998.
21. C. Solomons, T. W. Graham Fryhle, *Organic Chemistry*, Wiley, New York, 7th edn up., 2001.
22. J. Wu, G. Yue, Y. Xiao, H. Ye, J. Lin, and M. Huang, *Electrochim. Acta*, 2010, **55**, 5798–5802.

23. S. Abdulalmohsin and J. B. Cui, *J. Phys. Chem. C*, 2012, **116**, 9433–9438.
24. T. Chen, X. Wu, and R. D. Rieke, *J. Am. Chem. Soc*., 1995, **117**, 233–244.
25. M. S. A. Abdou and S. Holdcroft, *Macromolecules*, 1993, **26**, 2954–2962.
26. T. E. Conners and S. Banerjee, *'X-ray Photoelectron Spectroscopy' in 'Surface Analysis of Paper'*, CRC press, Boca Raton, 1995.
27. C. J. Schaffer, C. M. Palumbiny, M. a Niedermeier, C. Jendrzejewski, G. Santoro, S. V Roth, and P. Müller-Buschbaum, *Adv. Mater*., 2013, **25**, 6760–6764.
28. S. Yu, G. Santoro, K. Sarkar, B. Dicke, P. Wessels, S. Bommel, R. Do, J. Perlich, M. Kuhlmann, E. Metwalli, J. F. H. Risch, M. Schwartzkopf, M. Drescher, P. Müller-Buschbaum, and S. V Roth, J. *Phys. Chem. Lett*., 2013, **4**, 3170–3175.
29. M. Al-Hussein, M. Schindler, M. a Ruderer, J. Perlich, M. Schwartzkopf, G. Herzog, B. Heidmann, A. Buffet, S. V Roth, and P. Müller-Buschbaum, *Langmuir*, 2013, **29**, 2490–2497.

For table of contents use:
P3HT degradation is shown to be suppressed when it is on conductive substrates. This 'substrate effect' is more significant than maintaining an inert environment.